

Modeling of Multicomponent Reactive Systems

D. Anders, K. Weinberg

In recent engineering applications reaction-diffusion systems obtain more and more importance for the production and design of functional materials. Therefore, in this contribution spinodal decomposition in multicomponent systems subjected to chemical reactions is studied. To this end, the classical Cahn-Hilliard phase field model is extended by additional contributions from chemical reactions. After deriving the reaction-diffusion model in a thermodynamically consistent way, for the first time a numerical simulation of a ternary chemically reactive phase separating system is presented.

1 Introduction into Reaction-Diffusion Systems

Clearly, chemical reactions play a crucial role in our every-day life. Indeed, there is a multifaceted range of chemical reactions such as oxidation/corrosion of metals, combustion, chemical reactions in human metabolism or photochemical reactions like photosynthesis just to mention a few of them. The main feature about chemical reactions is their competency to generate substances which usually have properties different from their reactants. This property can be exploited for structural optimization of multicomponent systems susceptible to chemical reactions. To us chemical reactions are a special matter of interest because they are able to influence the microstructure in multicomponent functional systems. It is commonly known that the microstructural arrangement determines the macroscopic material behavior. In this context, the evolving microstructure profoundly affects the structural properties, life expectation and reliability of the whole system. For this reason, our goal is to provide an insight into the effect of chemical reactions on microstructure by studying so-called *reaction-diffusion* systems. As the name implies, a reaction-diffusion system is driven by diffusion phenomena and local chemical reactions. To understand the processes in reaction-diffusion systems, it is therefore crucial to introduce the essential conceptions of chemical reactions and their kinetics. Subsequently, we will couple diffusion and chemical reactions to arrive at the framework of phase-separating reaction-diffusion systems.

1.1 Chemical Reactions and Fundamentals of their Kinetics

A chemical reaction is formally defined as a process that induces an interconversion of chemical species. Classically, chemical reactions are subdivided into *elementary reactions* and *stepwise/composite reactions*. While elementary reactions form a class of simplest reactions, stepwise/composite reactions encompass at least one reaction intermediate involving at least two consecutive elementary reactions, see (Müller, 1994, p. 1167).

By definition, the symbolic representation of a chemical reaction is given in such a manner that the reactant entities are constituted on the left hand side and the product entities are written on the right hand side. The coefficients multiplying the chemical symbols and formulae of entities are the so-called stoichiometric coefficients. Different symbols are used to connect the reactants and products with the following meanings:

- The symbol \rightarrow is used for a stoichiometric relation with a net forward reaction.
- The symbol \rightleftharpoons specifies a stoichiometric relation with a reaction in both directions.
- The symbol \rightleftharpoons is employed for the stoichiometric relation of an equilibrated chemical reaction.

See also (Green Book, 1993, p. 45) for further reference. For example, let us consider a typical binary chemical reaction

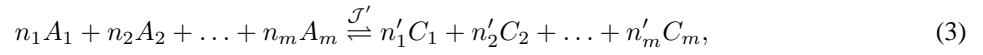


in which n_A moles of molecules of type A and n_B moles of molecules labeled B react to produce n_C moles of molecules of type C and n_D moles of molecules labeled D . In this example the coefficients n_i represent the stoichiometric coefficients for molecules A , B , C and D , respectively. The (positive) parameter \mathcal{J} represents here the reaction rate of the respective chemical reaction. The reaction rate is employed to give information on the kinetics of a chemical reaction. For example, corrosion (oxidation) of alloys under the atmosphere is a slow reaction which can take many years, whereas combustion is an extremely fast reaction.

The abovementioned reaction rate \mathcal{J} is usually addressed by a phenomenological rate law, which expresses that \mathcal{J} depends on the amount of each reactant in a reacting mixture, giving for our model reaction (1) the rate equation:

$$\mathcal{J} = k [A]^\alpha [B]^\beta, \quad (2)$$

where $[A]$ and $[B]$ express the amount concentration of the species A and B , respectively. The positive proportionality constant k , independent of $[A]$ and $[B]$, is referred to as rate constant/coefficient. The constant exponents α and β are independent of concentration and time, cf. (Müller, 1994, p. 1147). According to (Cross and Greenside, 2009, p. 111) the exponents in the rate equation of an elementary reaction are given by the corresponding stoichiometry factors. If we regard our exemplary reaction (1) as an elementary reaction this will mandate $\alpha = n_A$ and $\beta = n_B$. Please note that in general α and β cannot be identified with the respective stoichiometric coefficients of the balanced stoichiometric relation. All parameters of the rate equation have to be determined experimentally. In the scope of this work we will focus on elementary equilibrium/opposed reactions of type



where \mathcal{J}' denotes the overall reaction rate which follows from the difference between the forward and backward reaction rates according to

$$\mathcal{J}' = k_{+1} \prod_{i=1}^m [A_i]^{n_i} - k_{-1} \prod_{i=1}^m [C_i]^{n'_i}. \quad (4)$$

Here we introduced k_{+1} as the rate coefficient characterizing the reaction that consumes the species A_i for $i = 1, \dots, m$; k_{-1} characterizes the rate coefficient for the backward reaction, which consumes the quantities C_i and in return it produces A_i (for $i = 1, \dots, m$). Now we have presented the basic conceptions and equations to capture the kinetics of elementary chemical reactions, which will be employed in the derivation of the evolution equations for reaction-diffusion systems.

1.2 Thermodynamical Model for Reaction-Diffusion Systems

In this section we will follow ideas from de Groot and Mazur (1962) and use the previously obtained results for chemical reactions to couple them to diffusion phenomena. As outlined in (Cross and Greenside, 2009, p. 111) the evolution of concentration in a multicomponent reaction-diffusion system is driven by two competitive mechanisms, namely chemical reactions and diffusion processes. According to the results from the previous section, chemical reactions alter the local concentrations of their reactants and products following a concentration dependent rate law. However, diffusion decreases spatial gradients of concentration profiles, in such a manner that a mass transport takes place from regions of high concentration to regions of smaller concentration values.

Mathematically these competing mechanisms are captured within generalized phenomenological evolution equations for multicomponent systems consisting of n components, which undergo r reactions according to

$$\rho \frac{dc_k}{dt} = -\nabla \cdot \mathbf{J}_k + \sum_{j=1}^r v_{kj} \bar{\mathcal{J}}_j, \quad (k = 1, \dots, n), \text{ in } \Omega \times [0, T] \quad (5)$$

$$\text{with } \rho = \sum_{k=1}^n \rho_k \text{ and } c_k = \frac{\rho_k}{\rho}. \quad (6)$$

Note that $d(\bullet)/dt = \partial(\bullet)/\partial t + \mathbf{v} \cdot \nabla(\bullet)$ denotes the substantial time derivative with the barycentric velocity field \mathbf{v} . In Eq. (5) ρ denotes the total mass density and ρ_k is the mass density of the k th component. The scalar fields c_k characterize the mass fractions (concentration) of the respective components. In general, Eq. (5) expresses the conservation of mass, where the temporal evolution of the concentration fields c_k is affected by an interplay between the corresponding diffusive mass current \mathbf{J}_k and a source term $\sum_{j=1}^r v_{kj} \bar{\mathcal{J}}_j$ due to chemical reactions. In our notation $\bar{\mathcal{J}}_j$ denotes a generalized chemical reaction rate of the j th reaction.

Please note that an application of the mass concentration as evolution variable to describe the local composition

of our system demands the classical reaction rate \mathcal{J} , which is originally formulated in molar concentrations, to be adjusted in its dimension in order to fit Eq. (5). The prerequisite calculations will be performed in a later part of this passage. The coefficient v_{kj} divided by the molecular mass M_k of component k is proportional to the stoichiometric coefficient of the k th chemical substance in the j th chemical reaction. By convention, coefficients v_{kj} are counted positive if k th chemical substance is produced within the j th chemical reaction; and negative if the k th substance is consumed in reaction j .

Since mass conservation has to be guaranteed in each separate chemical reaction, it holds

$$\sum_{k=1}^n v_{kj} = 0, \quad (j = 1, 2, \dots, r). \quad (7)$$

For mathematical reasons it is convenient to normalize the coefficients v_{kj} in such a manner that for the reactants ($k = 1, 2, \dots, q_j$) of each reaction j it holds

$$\sum_{k=1}^{q_j} v_{kj} = -1, \quad (j = 1, 2, \dots, r). \quad (8)$$

In view of the mass conservation (7) and the normalization (8) we obtain a normalization for the products ($k = q_j + 1, q_j + 2, \dots, n$) given by

$$\sum_{k=q_j+1}^n v_{kj} = 1, \quad (j = 1, 2, \dots, r). \quad (9)$$

In the scope of this manuscript we will only consider incompressible reaction-systems, which do not change their volume in chemical reactions. Under these restrictions the total mass density ρ is constant in time and therefore we may rewrite the kinetic quantities of chemical reactions in terms of (mass) concentration. To this end we employ the relation

$$[X_i] = \frac{\rho_i}{M_i} = \frac{\rho c_i}{M_i}, \quad (10)$$

where $[X_i]$ is the molar concentration of the i th component (in units of mol/m³), ρ_i denotes the partial density of component i (in units of kg/m³) and M_i is the respective molar mass of constituent i (in units of kg/mol). An application of (10) yields with the true stoichiometric coefficients n_{kj} and the conventional reaction rates \mathcal{J}_j

$$n_{kj} = \frac{a_j v_{kj}}{M_k} \text{ and } \mathcal{J}_j = \frac{\bar{\mathcal{J}}_j}{a_j}, \quad (11)$$

where the proportionality constants a_j (in units of kg/mol) can be deduced from the normalization conditions (8) and (9) as

$$a_j = \sum_{k=q_j+1}^n n_{kj} M_k = - \sum_{k=1}^{q_j} (-n_{kj}) M_k. \quad (12)$$

According to the usual sign convention the stoichiometric coefficients of reactants are counted as negative, to indicate that the corresponding substances are consumed during reaction. Now we are able to employ the rate equation (4) to obtain a general expression for the reaction rate of each elementary reaction considered in our reaction-diffusion system

$$\mathcal{J}_j = k_{+1,j} \prod_{k=1}^{q_j} [X_k]^{n_{kj}} - k_{-1,j} \prod_{k=q_j+1}^n [X_k]^{n_{kj}}. \quad (13)$$

In contrast to the convention in Eq. (12), there is no negative sign in the exponent of the product of reactants results. In this way it is guaranteed that the exponents in our rate law are always positive as it was introduced in the general formalism (4). By means of relations (11), (12) and (13) we are able to give a consistent representation of the generalized chemical reaction rate $\bar{\mathcal{J}}_j$ and the scaled stoichiometric coefficients v_{kj} .

Let us now take into account that in the case of generalized Fickian diffusion the diffusive mass current \mathbf{J}_k of component k is given by

$$\mathbf{J}_k = -\rho \mathbf{M} \nabla \mu_k = -\rho \mathbf{M} \nabla \left(\frac{\delta F}{\delta c_k} \right), \quad (14)$$

where \mathbf{M} is the mobility tensor and μ_k denotes the chemical potential with respect to the k th component. The system's Helmholtz free energy is given by

$$F(c_1, c_2, \dots, c_n, T) = \int_{\Omega} (\Psi^{\text{con}} + \Psi^{\text{int}}) \, d\Omega \quad (15)$$

involving a configurational and interfacial energy contribution. For a multiphase mixture the configurational free energy density Ψ^{con} is given by

$$\Psi^{\text{con}}(T, p, c_1, \dots, c_n) = \sum_{i=1}^n g_i^0(T, p) c_i + \theta(T) \sum_{i=1}^n c_i \ln c_i + \frac{1}{2} \sum_{\substack{1 \leq i, j \leq n \\ i \neq j}} c_i c_j \chi_{ij}^{(0)}, \quad (16)$$

where $g_i^0(T, p)$ are the Gibbs free energy densities of the pure i th component and the second part accounts for energy contributions from the entropy of mixing. The entropy contribution is multiplied by the temperature depended material parameter θ . The first two energy contributions represent the classical Lewis-Randall ideal solution model. For the consideration of reasonable solutions, which generally show a non-ideal behavior, it is crucial to include the third term into the energy representation involving a Porter's type excess energy contribution (see O'Connell and Haile, 2005).

The interfacial free energy density Ψ^{int} accounts for the nonlocal effect of surface tension which is related to surface energy density contained within the interfacial regions between different phases. It is formally given by

$$\Psi^{\text{int}} = \sum_{i=1}^n \frac{\kappa_i}{2} \|\nabla c_i\|^2, \quad (17)$$

where the material parameters κ_i are related to surface energy density γ and thickness l of the interfacial layers between the domains of each phase. Finally, the evolution equations for chemically active multicomponent reaction-diffusion systems read

$$\rho \frac{dc_k}{dt} = \nabla \cdot (\rho \mathbf{M} \nabla \mu_k) + \sum_{j=1}^r v_{kj} \bar{J}_j, \quad (k = 1, \dots, n), \quad \text{in } \Omega \times [0, T]. \quad (18)$$

The boundary conditions are given in the usual manner, such that

$$\mathbf{J}_k \cdot \mathbf{n} = 0 \text{ and } \nabla c_k \cdot \mathbf{n} = 0, \quad (k = 1, \dots, n), \quad \text{on } \partial\Omega \times [0, T], \quad (19)$$

where \mathbf{n} is the unit outward normal on $\partial\Omega$. As initial boundary condition, we employ

$$c_k(\mathbf{x}, 0) = c_{k,0}(\mathbf{x}) \quad (20)$$

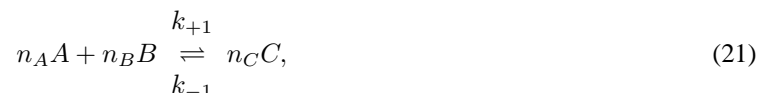
The introduced formulation of evolution equations expressing mass continuity for reaction-diffusion systems (18) may also be found in a similar form in de Groot and Mazur (1962).

2 Computational Studies of Multicomponent Reaction-Diffusion Systems

In the sequel, we will demonstrate computational studies of a representative ternary system subjected to an interfacial chemical reaction coupled with diffusion phenomena such as phase separation and microstructural coarsening. Such a kind of chemical reaction was experimentally studied by Horiuchi et al. (1997) to adjust morphologies in ternary immiscible polymer blends.

To keep the computational cost at a reasonable level we will consider here only one representative system, which suffices to illustrate the essential physics underlying the phenomena in chemically activated phase-separating materials. Following the spirit of Glotzer et al. (1995) we focus in this work on solid mixtures which are quenched into a thermodynamically unstable state simultaneously undergoing an elementary chemical reaction. However, the operative chemical reaction is regarded as an externally induced/controlled processes due to external fields, e.g. irradiation.

Although computational studies of binary reaction-diffusion systems can be employed to show the basic traits of chemically reactive systems as done by Glotzer et al. (1995), they are rather academic because chemical reactions usually involve multiphase mixtures. In our considerations we regard an evolution scenario within an unstable ternary system consisting of species A , B and C , which is simultaneously subjected to the bimolecular reaction



where k_{+1} and k_{-1} are according to our notation the rate coefficients of the forward reaction $n_A A + n_B B \rightarrow n_C C$ and the backward reaction $n_C C \rightarrow n_A A + n_B B$, respectively. The corresponding reaction rate \mathcal{J}_1 reads according to the general form (4)

$$\mathcal{J}_1 = k_{+1} [A]^{n_A} [B]^{n_B} - k_{-1} [C]^{n_C}. \quad (22)$$

The microstructural evolution of this ternary mixture is captured by the temporal evolution of the mass fractions $c_1 := c_A$ and $c_2 := c_B$. The mass concentration c_3 of component C follows from the overall mass conservation law

$$c_1 + c_2 + c_3 = 1 \quad \Leftrightarrow \quad c_3 = 1 - (c_1 + c_2).$$

According to the general evolution equations for multiphase reaction-diffusion systems (18) we obtain the ternary evolution equations

$$\frac{\partial c_1}{\partial t} = \nabla \cdot (\mathbf{M} \nabla \mu_1) - n_A M_A \bar{k}_{+1} c_1^{n_A} c_2^{n_B} + n_A M_A \bar{k}_{-1} (1 - (c_1 + c_2))^{n_C}, \quad (23)$$

$$\frac{\partial c_2}{\partial t} = \nabla \cdot (\mathbf{M} \nabla \mu_2) - n_B M_B \bar{k}_{+1} c_1^{n_A} c_2^{n_B} + n_B M_B \bar{k}_{-1} (1 - (c_1 + c_2))^{n_C}, \quad (24)$$

$$\frac{\partial c_3}{\partial t} = \nabla \cdot (\mathbf{M} \nabla \mu_3) + n_C M_C \bar{k}_{+1} c_1^{n_A} c_2^{n_B} - n_C M_C \bar{k}_{-1} c_3^{n_C}. \quad (25)$$

Since the concentration profile c_3 can be calculated from the concentrations c_1 and c_2 , we need only to solve Eqs. (23) and (24). Please note that we employ here an averaged overall mobility tensor \mathbf{M} that captures the kinetics of the diffusion contribution within the evolution equations. The coefficients \bar{k}_{+1} and \bar{k}_{-1} denote scaled rate coefficients, which follow from the normalization conditions (8) and (9).

For the numerical solution of the ternary evolution equations (23)-(25) we employ a B-spline based finite element approach for spatial discretization and a classical Crank-Nicholson scheme for temporal discretization. To get a profound insight into the mathematical details on the application of these discretization schemes the authors refer to their original papers on the treatment of similar Cahn-Hilliard type phase-field equations (cf. Anders and Weinberg, 2011a; Anders et al., 2011; Anders and Weinberg, 2011b).

Without loss of generality we assume for the diffusion dominated contributions an averaged, isotropic and constant mobility given by $\mathbf{M} = M \cdot \mathbf{I}$. The gradient coefficients κ_i of the individual phases are regarded as almost equal and they are represented by an overall gradient coefficient κ . For the multicomponent configurational energy density Ψ^{con} in Eq. (16) and the system parameters M, κ we employ the following dimensionless parameter set

$$M = 1, \quad \kappa = 2.5 \cdot 10^{-5}, \quad \theta(T) = 0.35, \quad \chi_{12}^{(0)} = \chi_{13}^{(0)} = \chi_{23}^{(0)} = 1.2. \quad (26)$$

These material parameters represent a thermodynamically unstable mixture which will decompose into three equilibrium phases. The corresponding shape of the configurational energy within the Gibbs triangle is illustrated in Fig. 1. This figure shows that the configurational energy has three local minima, which can be connected by a common tangent plane. The locus of these minima characterizes the composition of the equilibrium phases.

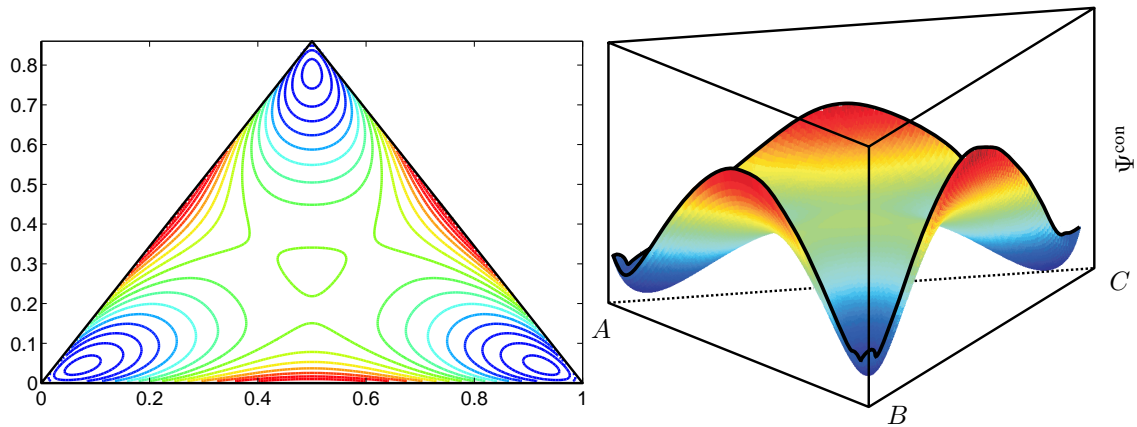


Figure 1: Contour plot and illustration of the shape of the configurational energy density Ψ^{con} . The blue color indicate low energy values and the red color marks high energy values.

Unfortunately, we suffer here from a lack of experimental reference data for the parameters of the chemical reaction. For this reason, we choose here rather academic stoichiometric coefficients

$$n_A = n_B = n_C = 1. \quad (27)$$

We assume that the molecular masses of substances A and B are similar ($M_A \approx M_B$) as it is often the case for chemically reactive polymer blends. From the computational point of view the individual molar masses are simply included into the scaled rate coefficients

$$\bar{k}'_{+1} := M_A \bar{k}_{+1} = M_B \bar{k}_{+1} \text{ and } \bar{k}'_{-1} := M_A \bar{k}_{-1} = M_B \bar{k}_{-1}. \quad (28)$$

In our simulations we make use of equal forward and backward reaction rates according to

$$\bar{k}'_{+1} = \bar{k}'_{-1} = 600. \quad (29)$$

Please keep in mind that our model is actually capable to reproduce other settings for chemical reactions.

Let us now come to the computational results for our representative ternary reaction-diffusion system. Here it should be emphasized that simulations of multicomponent reaction-diffusion systems are not common. To our knowledge, there exist no published computational studies of ternary chemically reactive phase-separating systems so far.

Our simulation initiates from a homogeneous state with slightly perturbed concentration profiles $\bar{c}_{A,0} = \bar{c}_{1,0} \approx 0.22$, $\bar{c}_{B,0} = \bar{c}_{2,0} \approx 0.21$ and $\bar{c}_{C,0} = \bar{c}_{3,0} \approx 0.57$. The system is arranged outside the chemical equilibrium. In the course of time, the system's microstructural evolution is dominated by the tendency to reach the chemical equilibrium, as it is also the case for the binary reaction-diffusion system. This trend is illustrated in the overall concentration evolution of the substances A , B and C in Fig. 2. We observe here a complete rearrangement of the system's composition. While the overall concentration of C decreases, the concentrations of A and B considerably increase with time. The equilibration of chemical reactions takes place in the time interval of $t = 0$ up to $t = 0.01$. This temporal interval is dyed in dark gray in Fig. 2. The later evolution stages are dominated by classical coarsening effects.

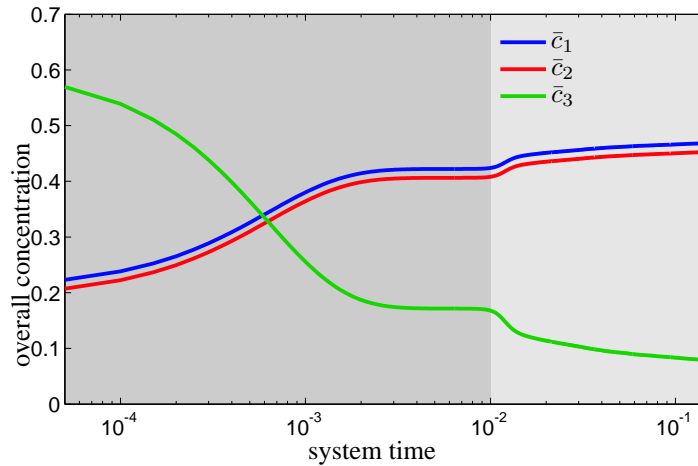


Figure 2: Temporal evolution of the overall concentrations $\bar{c}_1 = \bar{c}_A$, $\bar{c}_2 = \bar{c}_B$ and $\bar{c}_3 = \bar{c}_C$ of the chemical species A , B and C , respectively.

The morphologies observed during our computational studies exhibit the so-called *capsule formation*, where phases are encapsulated by a thin layer of another phase, see Figs.3 and 4. The simulated micrographs indicate that the initially homogeneous ternary mixture at first rearranges into chemical equilibrium before separation into three equilibrium phases takes place. Due to the altered overall average concentrations of substances A , B and C , the evolving microstructure is dominated by a lamellar pattern. This structure is induced by the two equivalent A -rich and B -rich major phases. In the computational micrographs the A -rich phase is characterized by light brown domains and the B -rich phases are dyed in neon green, see Figs.3 and 4. The third C -rich equilibrium phase (reddish domains) represents here the minor phase, which accumulates at the interfacial regions between the A - and B -rich lamellae. The reason for this accumulation of C -type matter at the interfaces leading to an encapsulation of the major phases is fully induced by chemical reactions. Since we simulate diffusion phenomena subjected to a chemical reaction which requires matter of A and B in order to produce C , the chemical reaction is concentrated at the interfacial regions, where A and B simultaneously occur. In the bulk regions, where there is a

constantly high amount of A and a lack of B and vice versa, the chemical reaction is complicated by a lack of one reactant. This special kind of morphology formation was experimentally observed by Horiuchi et al. (1997).

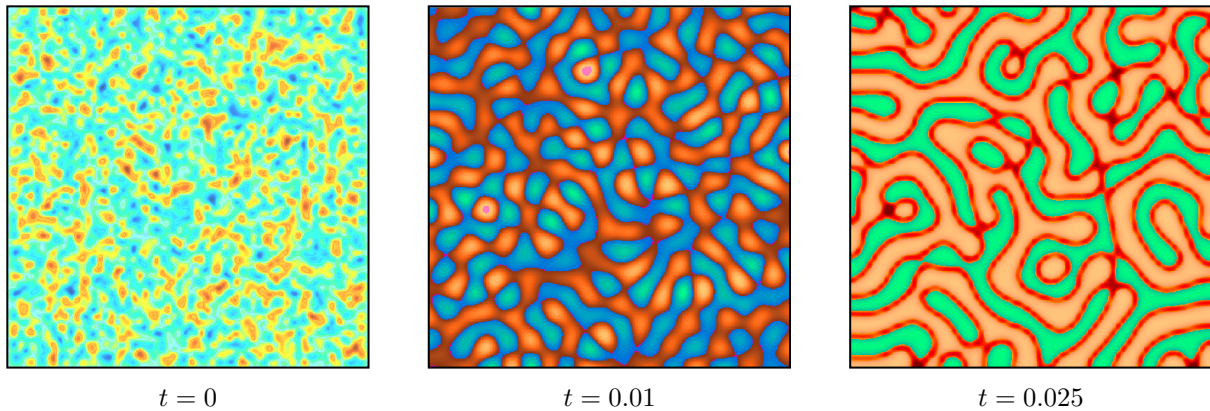


Figure 3: Morphology evolution in a ternary reaction-diffusion system at early stages.

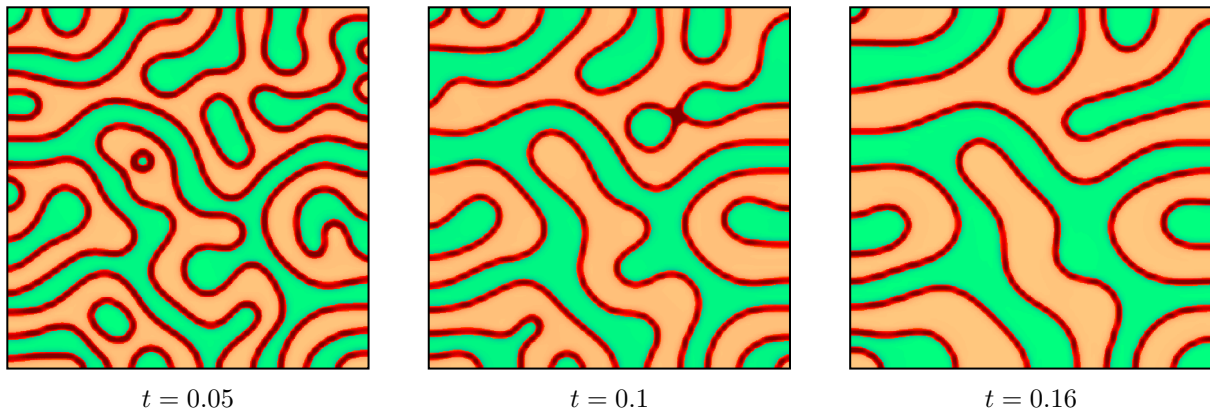


Figure 4: Morphology evolution in a ternary reaction-diffusion system at later stages.

Other computational studies with different initial settings indicated that the obtained results are invariant under modifications of the initial concentration. Classical non reactive phase-separating mixtures usually exhibit a microstructural formation which inherently depends on their initial configuration. For chemically active systems this is actually not the case. It shows that the microstructure of multicomponent systems can be forced by chemical reactions out of its original arrangement into a capsule formation or other types of microstructural formation.

3 Summary

In this work a thermodynamically consistent model for multicomponent phase-separating reaction-diffusion systems is presented. Our approach takes into account the complete coupling between chemical reactions and diffusion events on the microscopic level. The performed simulation results corroborate the idea that chemical reactions may be used as an effective tool to exert control on the microstructure in functional materials. It shows that our model is basically capable to reproduce the experimentally observed microstructural evolution in ternary polymer blends driven by interfacial reactions, as shown in Horiuchi et al. (1997).

References

- Anders, D.; Weinberg, K.: Numerical simulation of diffusion induced phase separation and coarsening in binary alloys. *Int. J. of Computational Materials Science*, 50, (2011a), 1359 – 1364.
- Anders, D.; Weinberg, K.: A variational approach to the decomposition of unstable viscous fluids and its consistent numerical approximation. *ZAMM - Journal of Applied Mathematics and Mechanics*, 91, (2011b), 609 – 629.
- Anders, D.; Weinberg, K.; Reichardt, R.: Isogeometric analysis of thermal diffusion in binary blends. *Int. J. of Computational Materials Science*, (online version at <http://dx.doi.org/10.1016/j.commatsci.2011.01.008>).

Cross, M.; Greenside, H.: *Pattern formation and dynamics in nonequilibrium systems*. Cambridge University Press, Cambridge (2009).

de Groot, S.; Mazur, P.: *Non-equilibrium thermodynamics*. North-Holland, Amsterdam (1962).

Glotzer, S.; Di Marzio, E.; Muthukumar, M.: Reaction-controlled morphology of phase-separating mixtures. *Physical Review Letters*, 74, (1995), 2034 – 2037.

Green Book, .: *IUPAC Quantities, Units and Symbols in Physical Chemistry. Second Edition*. Blackwell Scientific Publications, Oxford (1993).

Horiuchi, S.; Matchariyakul, N.; Yase, K.; Kitano, T.: Morphology development through an interfacial reaction in ternary immiscible polymer blends. *Macromolecules*, 30, (1997), 3664 – 3670.

Müller, P.: Glossary of terms used in physical organic chemistry (IUPAC recommendations 1994). *Pure & Appl. Chem.*, 66, (1994), 1077 – 1184.

O’Connell, J.; Haile, J.: *Thermodynamics: Fundamentals for Applications*. Cambridge University Press, Cambridge (2005).

Address: M.Sc. Denis Anders and Prof. Dr.-Ing. Kerstin Weinberg, Lehrstuhl für Festkörpermechanik, Universität Siegen, D-57068 Siegen.

email: anders@imr.mb.uni-siegen.de; weinberg@imr.mb.uni-siegen.de .